*Zoological Journal of the Linnean Society*, 2022, **195**, 106–124. With 4 figures.

# The evolution of tinamous (Palaeognathae: Tinamidae) in light of molecular and combined analyses

FRANCISCA C. ALMEIDA[1], ANA L. PORZECANSKI[2], JOEL L. CRACRAFT[2] and SARA BERTELLI[2,3,4,*]

[1]*Instituto de Ecología, Genética y Evolución (IEGEBA), Consejo Nacional de Investigaciones Científicas y Tecnológicas (CONICET) / Universidad de Buenos Aires (UBA), Ciudad Autónoma de Buenos Aires, Argentina*
[2]*American Museum of Natural History, 200 Central Park West, New York, NY, 10024-5102, USA*
[3]*Fundación Miguel Lillo (FML), Miguel Lillo 251, 4000 San Miguel de Tucumán, Argentina*
[4]*Unidad Ejecutora Lillo (UEL) - Consejo Nacional de Investigaciones Científicas y Tecnológicas (CONICET), San Miguel de Tucumán, Tucumán, Argentina*

*Received 12 March 2021; revised 24 July 2021; accepted for publication 25 August 2021*

The Neotropical tinamous are of particular interest in our efforts to understand the evolution of modern birds. They inhabit both forested and open environments and, although volant, have limited flight capabilities. Numerous studies have recognized the monophyly of tinamous and their relationships either as sister to the flightless ratites (ostriches, emus and their relatives) or within the ratites themselves. Despite the numerous bird phylogenies published recently, modern investigations of relationships within the tinamous themselves have been limited. Here, we present the first detailed phylogenetic analysis and divergence-date estimation including a significant number of tinamou species, both extant and fossil. The monophyly of most currently recognized polytypic genera is recovered with high support, with the exception of the paraphyletic *Nothura* and *Nothoprocta*. The traditional subdivision between those tinamous inhabiting open areas (Nothurinae) and forest environments (Tinaminae) is also confirmed. A temporal calibration of the resultant phylogeny estimates that the basal divergence of crown Tinamidae took place between 31 and 40 Mya.

ADDITIONAL KEYWORDS: combined analyses – molecular dating – Nothurinae – phenotypic evolution – phylogeny – Tinaminae.

## INTRODUCTION

Tinamous are a distinctive family of Neotropical birds within the subclass Palaeognathae. Several aspects of their biology make them of high interest in the study of bird evolution. Tinamous are widespread geographically and are associated with a variety of habitats from southern Mexico to Patagonia, inhabiting both forested and open environments (Cabot, 1992; Davies, 2002). Although volant, the flight capabilities of these birds are limited; they produce distinctive songs and have notably colourful eggs (Davies, 2002). Numerous studies have recognized the monophyly of tinamous and their relationships to the flightless ratites (ostriches, emus and their relatives), placing both groups together in the Palaeognathae Pycraft, 1900, the sister clade to all other extant birds (Neognathae Pycraft, 1900) (Cracraft, 1974; Livezey & Zusi, 2007; Hackett *et al.*, 2008; Harshman *et al.*, 2008; Bourdon *et al.*, 2009; Haddrath & Baker, 2012; Worthy & Scofield, 2012; Smith *et al.*, 2013; Jarvis *et al.*, 2014; Mitchell *et al.*, 2014; Claramunt & Cracraft, 2015; Prum *et al.*, 2015). Phylogenetic analyses based on molecular data and including fossil taxa have revealed that tinamous are closely related to the moas of New Zealand, contradicting a previous hypothesis based on biogeography that suggested they were related to the South American rheas (Mitchell *et al.*, 2014, Yonezawa *et al.*, 2017). More recent studies based on phylogenomic data or on the supertree approach have corroborated the results of these previous molecular studies (Cloutier *et al.*, 2019; Kimball *et al.*, 2019; but see Reddy *et al.*, 2017).

*Corresponding author. E-mail: sbertelli@lillo.org.ar

Despite the growing use of molecular data in phylogenetic studies, until now only one study has included molecular data from a significant number of tinamou species, and it reported only preliminary results (Bertelli & Porzecanski, 2004). Hence, most published hypotheses for the relationships within Tinamidae have been based on external morphology (Bertelli *et al.*, 2002; Bertelli & Giannini, 2013) and internal anatomy (Bertelli & Chiappe, 2005; Bertelli *et al.*, 2014). A more recent and inclusive phenotype-based phylogenetic study of all extinct and living species of tinamous (Bertelli, 2017) supported the monophyly of the subfamilies proposed by Miranda Ribeiro (1938): the forest Tinaminae (*Crypturellus* Brabourne & Chubb, 1914, *Nothocercus* Bonaparte, 1856 and *Tinamus* Hermann, 1783) and the open-area Nothurinae (*Eudromia* I. Geoffroy Saint-Hilaire, 1832, *Nothoprocta* Sclater & Salvin, 1873, *Nothura* Wagler, 1827, *Rhynchotus* Spix, 1825, *Taoniscus* Gloger, 1842 and *Tinamotis* Vigors, 1837).

Here, we review the interrelationships of tinamous based on phenotypic data and new molecular data from three mitochondrial and five nuclear loci, extending the previously published phylogenetic analysis of the taxa based on phenotypic data alone (Bertelli, 2017). The resulting phylogeny is used to evaluate patterns of diversification within the group, including the hypothesis of Miranda Ribeiro (1938) of an early split into forest and non-forest lineages, and to calibrate the tinamou phylogeny based on fossil evidence. The data were analysed separately and in combination; the scoring of osteological characters allowed us to include extinct members of the group. Hence, we were able not only to discuss morphological changes in the context of the current phylogenetic hypothesis, but also to shed light on the question of the timing of their diversification, which varies considerably depending on the fossil calibration. Thus, we were able to test previously proposed hypotheses and produce a more robust reconstruction of the phylogenetic interrelationships of tinamids and to highlight specific areas and questions in need of further research.

## MATERIAL AND METHODS

### Sampling

The molecular matrix included 32 of the 45 currently recognized tinamou species, including at least one species per genus. All 32 species were represented by mitochondrial sequences, whereas 19 also included sequences of at least one nuclear gene (see Supporting Information, Table S1). In the combined, total evidence analysis, we used the same extant terminal taxa as in the study by Bertelli (2017), which comprised all currently recognized extant species plus some morphologically diagnosable forms that have not been recognized as distinct species but do correspond, in some cases, to populations previously assigned subspecific status. One exception was *Crypturellus duidae* (Zimmer, 1938), which is considered a subspecies of *Crypturellus erythropus* (Pelzeln, 1863) by some authors and was excluded from the matrix owing to the large amount of missing data (scorings for only external morphology) that rendered its taxonomic position unresolvable. Hence, although the dataset used in this study is limited in terms of molecular loci (in comparison with genome-level studies), it is one of the most comprehensive in terms of species representation.

Given that the placement of Tinamidae in Palaeognathae has been consistently supported (Hackett *et al.*, 2008; Jarvis *et al.*, 2014; Claramunt & Cracraft, 2015; Prum *et al.*, 2015), we also included sampling of extant ratites as outgroups [*Apteryx australis* Shaw, 1813, *Apteryx haastii* Potts, 1872, *Apteryx rowi* Tennyson *et al.*, 2003, *Apteryx owenii* Gould, 1847, *Casuarius bennetti* Gould, 1857, *Casuarius casuarius* (Linnaeus, 1758), *Dromaius novaehollandiae* (Latham, 1790), *Pterocnemia pennata* d'Orbigny, 1837, *Rhea americana* (Linnaeus, 1758) and *Struthio camelus* Linnaeus, 1758], in addition to recently extinct moas [*Anomalopteryx didiformis* (Owen, 1844), *Emeus crassus* (Owen, 1846), *Emeus curtus* (Owen, 1846), *Dinornis robustus* (Owen, 1846), *Megalapteryx didinus* (Owen, 1883) and *Pachyornis australis* (Oliver, 1949)] and elephant birds (*Aepyornis hildebrandti* Burckhardt, 1893 and *Mullerornis agilis* Milne-Edwards & Grandidier, 1894). Additionally, galliform [*Gallus gallus* (Linnaeus, 1758)] and anseriform (*Chauna torquata* Oken, 1816) taxa were added to the analysis as outgroups to palaeognaths because they are widely accepted as early divergences in Neognathae (Hackett *et al.*, 2008; Jarvis *et al.*, 2014; Claramunt & Cracraft, 2015; Prum *et al.*, 2015). Finally, fossil taxa were included in the combined analysis to assess their phylogenetic positions and to determine node-based calibration points for the molecular-clock dating analysis. Representing the ingroup, we included the fossil taxa *Eudromia* sp., *Eudromia olsoni* Tambussi & Tonni, 1985, *Nothura parvula* (Brodkorb, 1963) and two undescribed fragments of coracoids (MACN-SC3610 and MACN-SC 3613; Bertelli *et al.*, 2014). Other fossil taxa were excluded because preliminary analysis showed that their phylogenetic placement was unstable (including *Cypturellus reai* Chandler, 2012 and *Nothura* sp.; results not shown) as in the study by Bertelli *et al.* (2014). We also included taxa representing Lithornithidae, using the coding for two species (*Lithornis celetius* Houde, 1988 and *Lithornis vulturinus* Owen, 1840; following Bertelli *et al.*, 2014).

### Molecular data

Our molecular data consisted of three mitochondrial loci, namely cytochrome *b* (*Cytb*), cytochrome oxidase I (*COI*) and NADH dehydrogenase 2 (*ND2*), in addition to five nuclear loci, namely recombination activating 2 (*RAG2*), transforming growth factor beta 2 (*TGFB*), tropomyosin 1 (*TPM1*), muscle-specific receptor tyrosine-protein kinase (*MUSK*) and fibrinogen gene (*FIB7*). The nuclear loci consisted mostly of intronic sequences, except for one locus (*RAG2*). Tinamou sequences of the *RAG2* and *Cytb* genes were obtained and used in a previous, preliminary analysis (Porzecanski, 2003; Bertelli & Porzecanski, 2004).

Tissue samples were obtained from field collections in Bolivia and Uruguay, from museum tissue collections and from toe pads of museum study skins (voucher information with GenBank accession numbers is provided in Supporting Information, Table S1). Extraction and amplification protocols for fresh tissue samples followed Lee *et al.* (1997) and Cracraft *et al.* (1998), with specific primer design for several taxa, as necessary (see Porzecanski, 2003). In the case of museum skins, samples were collected following Mundy *et al.* (1997), and DNA was extracted using a Qiagen DNeasy tissue Extraction Kit (Qiagen) and amplified using capillary polymerase chain reactions (PCRs). All PCRs involving DNA from skins were performed using aerosol-resistant tips and taxon-specific primers for pieces of 250 bp in length and with a minimum of 50 bp overlap. Amplifications of the *ND2* gene and nuclear introns were done using primers and protocols described in the literature (Hackett, 1996; Primmer *et al.*, 2002; Zink *et al.*, 2006; Hackett *et al.*, 2008).

The DNA was sequenced using dye-terminator chemistry in an Applied Biosystems 377 automated sequencer following the manufacturer's recommendations. All portions of the sequence for each taxon were read in both directions, followed by sequence editing and assembly with SEQUENCHER v.4.1 software (Gene Codes, Ann Arbor, MI, USA). Complete match at > 50 bp overlap areas and reading frame maps were used to detect and prevent cases of cross-contamination or the amplification of nuclear products in the case of the skin samples.

Sequences from non-tinamid birds were obtained from GenBank. Each locus was aligned separately with MAFFT v.7 (Katoh & Standley, 2013), and all alignments were combined in matrices with MESQUITE 3.4 (Maddison & Maddison, 2018). The mitochondrial and nuclear matrices included a total of 2931 and 4385 bp and had 30 and 23% missing data in the ingroup, respectively. Partitioning schemes were evaluated with PARTITIONFINDER v.1.1.1 (Lanfear *et al.*, 2012) and considered both separate locus and codon positions in coding sequences of the mitochondrial genes and *RAG2* (Supporting Information, Table S2).

### Phenotypic data

The phenotypic matrix included a comprehensive taxonomic sampling, including all species of tinamous, which were scored for 249 characters from the integument (84) and internal anatomy (i.e. osteology and myology, 153) plus 12 characters from behaviour and breeding. Most of this matrix is similar to that built by Bertelli *et al.* (2017), considering primarily the phenotypic variation observed in Tinamidae, but some character descriptions and/or codings have been modified, and scorings for outgroup species were added (Supporting Information, Appendices S1 and S2). The external morphological characters included shape and colour patterns of the ramphotheca (horny sheath of the bill), podotheca (horny scales of legs) and natal and adult plumage; most of the plumage characters pertained to feather pigmentation patterns from different pterylae (feather tracts). Osteological and myological characters consisted of observed variations in cranial and postcranial structures (e.g. shape, relative development, presence/absence) of tinamous and outgroup taxa. Ethological characters were based mainly on the acoustic structure of songs, defined by quantitative (maximum and minimum frequency, range, etc.) and qualitative (syntactic structure, acoustics, modulation, etc.) variables that characterized each type of vocalization. Quantitative continuous characters representing different values of song frequencies (Bertelli & Tubaro, 2002) were analysed using the approach of Goloboff *et al.* (2008), in which each state is the numerical value observed in the species, and the transformation costs are the numerical differences between these values. Continuous characters were standardized such that the full range of variation was equivalent to one step of a discrete character (see Goloboff *et al.*, 2008). Reproductive and breeding characters (genitalia, oology and incubation) included phalli types, eggshell pigmentation and incubation of eggs (see Bertelli, 2017). The external morphological subset was 100% complete for the extant tinamou taxa and almost complete for other characters, such as behavioural, reproductive and breeding characters. The internal anatomy dataset was complete for almost 80% of extant terminals; the scoring was partial for the outgroup because some osteological or myological elements are absent or fused, obscuring assessment of homology. Several cases of non-comparability also occurred in plumage characters owing to uncertainty in primary homology of feather pigmentation characters in the outgroup

taxa (Bertelli, 2017). Missing data for fossil terminals ranged from 15% of osteology in the case of more complete specimens (such as *Lithornis* Owen, 1840) to 90% in the fragmentary Early Miocene tinamou taxa. The identification of the less well-preserved fossils was based on the presence of diagnostic apomorphies of Tinamidae (see Bertelli *et al.*, 2014).

### Phylogenetic analyses

We analysed nuclear and mitochondrial matrices separately and then combined the two in a large matrix. Finally, we analysed combined molecular and phenotypic data (Bertelli, 2017). For each molecular matrix, we ran maximum likelihood (ML), Bayesian inference (BI) and maximum parsimony (MP) searches. The ML searches were done with RAxML v.8.2.4 (Stamatakis, 2014) using 30 independent runs and the GTR+Γ substitution model, with parameters independently estimated for each data partition predetermined with PartitionFinder (see above). Branch support values were obtained with 1000 non-parametric bootstrap replicas. The BI searches were implemented with MrBayes v.3.2.6 (Ronquist & Huelsenbeck, 2003) using the best partition scheme and substitution models according to PartitionFinder (Supporting Information, Table S2). Standard searches were run for 10 million generations, sampling every 5000 trees. The first 20% of samples of each run were discarded as burn-in. Convergence of searches was assured by evaluating the potential scale reduction factor (~1.0) and effective sample size values (> 200) with the help of Tracer (Rambaut & Drummond, 2003). The MP searches were done with TNT v.1.5 (Goloboff *et al.*, 2008) using New Technology Searches, employing sectorial searches with 200 initial addition sequences being repeated until the shortest tree was found 20 times. Searches used ratchet and tree fusing and were followed by a final round of tree bisection–reconnection (TBR). Gaps were treated as missing characters. Statistical support for the nodes was obtained with 1000 replicates of non-parametric bootstrap and symmetric resampling (jackknife) analysis under the MP criterion.

We adopted two strategies to analyse molecular and morphological data together. The first strategy was the traditional one, in which the two dataset matrices were concatenated to generate a single matrix. This combined phenotypic plus molecular matrix included a total of 69 taxa and 7556 characters. Polymorphic states were coded as 'unknown' in combined searches based on ML and BI. In those searches, the evolutionary model was the optimal one according to PartitionFinder for the molecular data and the Mk model with ascertainment bias (Lewis, 2001) for the morphological data. For that analysis in RAxML, we used the commands *–f d –q partition_file.txt –K MK --asc_corr =lewis*, specifying the type ASC_MULTI for the morphological data in the partition file, whereas in MrBayes the model for the morphological data was set as *lset applyto = (x) nst = 1 coding = informative rates = gamma*.

The second strategy was based on the evolutionary placement algorithm (EPA; Berger *et al.*, 2011), which was proposed for the placement of samples for which a small number of scored characters is available on a tree obtained previously. This analysis was run in RAxML, using the ML tree obtained with the molecular dataset as a scaffold for the placement of taxa for which only morphological data were available. The command called the option *–f v –t molecular_tree.tre*, with the matrix and evolutionary models as described above for the concatenated analysis. The analysis was repeated with weights assigned to the morphological characters according to their congruence with the molecular data (a weight vector file was obtained with the command *–f u*, also with RAxML), but no differences in results were observed. Details about the treatment of the morphological characters are described in the Supporting Information (Appendix S2) and follow previous studies (Bertelli, 2017). The taxonomic distribution and optimization of characters under the MP criterion were implemented in TNT v.1.0 (Goloboff *et al.*, 2008).

### Molecular dating

We estimated the ages of nodes in the tinamou phylogeny using fossil calibrations and a Bayesian framework with BEAST 2 software v.2.3.1 (Bouckaert *et al.*, 2014). The molecular tree was calibrated using fossils that were located phylogenetically in both the outgroup and the ingroup. Outgroup fossils and their ages were assigned in accordance with recent avian molecular dating publications (Mitchell *et al.*, 2014; Claramunt & Cracraft, 2015; Prum *et al.*, 2015; Yonezawa *et al.*, 2017; Fig. 3; Table 1). Tinamid fossil-calibration constraints were used according to the phylogenetic positions determined in previous studies based on morphology (Bertelli *et al.*, 2014) and in the combined analysis of molecular and phenotypic data presented herein (see below). However, two alternative calibration schemes were used, differing in the assumption about the phylogenetic position of *Lithornis*. The volant lithornids from the Northern Hemisphere (Late Palaeocene to Middle Eocene) have been considered a sister group of Tinamidae by many authors (Houde, 1988; Bertelli, 2014; Mitchell *et al.*, 2014; Claramunt & Cracraft, 2015); this relationship was also recovered in our combined phylogenetic analysis under ML and MP. According to these results, we used

the age of the oldest lithornithid as a lower bound for the separation between moas and tinamids. In addition to the lithornithid age constraint, we also used five other calibration points: the estimated age of the crown Galloanserae (for which there is wide agreement in the literature); the age of *Emuarius* Boles, 1992 (Casuariformes); and the ages of three tinamid fossils (Table 1). Other authors have recently challenged the sister relationship between lithornithids and tinamids, suggesting that this presumed relationship is based on plesiomorphic characters and that lithornithids have a rather basal position within Palaeognathae (Worthy & Scofield, 2012; Nesbitt & Clarke, 2016). Based on this hypothesis, we performed a second analysis, eliminating the lithornithid age constraint and adding a constraint based on the age of *Diogenornis fragilis* Alvarenga, 1983, considered the oldest known rheiform (Alvarenga, 1983).

Dating analyses were based on the combined molecular matrix containing all loci analysed herein (mitochondrial, nuclear introns and *RAG2*), which allowed us to include a large number of tinamou species. Nevertheless, differences between mitochondrial and nuclear genes dating have been previously observed (Mitchell *et al.*, 2014), and the rapid evolutionary rates of tinamous may cause saturation problems especially in fast-evolving genes (e.g. Yonezawa *et al.*, 2017); therefore, we repeated the dating analysis using a matrix composed of slow-evolving *RAG2* sequences only. *RAG2* was the only nuclear gene for which we had exonic sequences, although those were available for only a subset of our tinamou samples.

Fossil ages were used as approximate minimum ages for their immediate ancestral nodes in the form of lower-bound priors of lognormal distributions. The lognormal distribution assigns the highest probability for node ages immediately before the fossil age, with a long tail of decreasing probabilities for older ages. We selected the clade defined by each calibrated node, set the age of the fossil as the offset and selected values for the mean and standard deviation of the lognormal distribution to give it a wide, yet realistic 95% confidence interval (Table 1). These calibrated nodes were constrained as monophyletic. We applied the uncorrelated local clock model and used the molecular matrices, which were partitioned as in the tree searches (Supporting Information, Table S2). Although the GTR+Γ model was assigned to all molecular partitions, parameter estimates were unlinked among partitions. We carried out two independent runs of 100 million generations, with trees sampled every 50 000 generations. Convergence of trees of Markov chain Monte Carlo steps was evaluated using TRACER v.1.6 (Rambaut *et al.*, 2014), combining the traces (after discarding the first 15% generations as burn-in) of each run. The number of generations was also sufficient to obtain an effective sample size > 200 for all parameters.

**Table 1.** Details on the fossil calibration used in the analysis of divergence dates

| Point | Calibration | Clade | Offset | *M* | *S* | Distribution | 95% Confidence Interval | Fossil | Evidence | Reference |
|---|---|---|---|---|---|---|---|---|---|---|
| 1 | Galloanserae | *Gallus* + *Chauna* | | 72.5 | 9 | Normal | 67.8–84.2 | – | Age estimate | Claramunt & Cracraft (2015) |
| 2 | *Emuarius* | *Dromaius* + *Casuarius* | 24 | 6 | 1 | Lognormal | 24.7–42.9 | *Emuarius guljaruba* Boles, 2001 | – | Worthy *et al.* (2014) |
| 3 | *Lithornis* | Tinamidae + Apeornithidae | 55 | 7 | 1 | Lognormal | 55.8–77.0 | *Lithornis celetius* Houde, 1988 | Phylogenetic analysis | Houde (1988); Bertelli *et al.* (2014); Mitchell *et al.* (2014) |
| 4 | *Diogenornis* | 'Higher ratites' (all but *Struthio*) | 55 | 7 | 1 | Lognormal | 55.8–77.0 | *Diogenornis fragilis* Alvarenga, 1983 | Synapomorphies with Rheidae | Alvarenga (1983) |
| 5 | *Eudromia* sp. | Nothurinae | 7 | 7 | 0.8 | Lognormal | 9.7–21.1 | *Eudromia* sp. Tambussi, 1987 | Phylogenetic analysis | Bertelli *et al.* (2014) |
| 6 | *Eudromia olsoni* | *Eudromia* + *Tinamotis* | 2.8 | 5 | 1 | Lognormal | 3.6–13.6 | *Eudromia olsoni* Tambussi & Tonni, 1985 | Phylogenetic analysis | Bertelli *et al.* (2014) |
| 7 | Tinaminae fossils | *Tinamus* + *Crypturellus* | 17 | 5 | 0.8 | Lognormal | 17.6–32.7 | MACNS 3610 and MACNS 3613 | Phylogenetic analysis | Bertelli *et al.* (2014) |

Offset, *M* and *S* are the parameters of the calibration prior distribution. Points 3 and 4 were used alternatively.

The summary tree was then visualized with FIGTREE v.1.4.2 (Rambaut, 2014).

## RESULTS

### MOLECULAR TREES

In general, both the mitochondrial and the nuclear analyses recovered the same major clades of tinamous as did the concatenated molecular tree (Fig. 1; Supporting Information, Figs S1, S2), with the major exceptions being observed in some relationships among species of *Crypturellus* and in the position of *Nothoprocta cinerascens* (Burmeister, 1860). The BI and ML trees resulting from analysis of the concatenated molecular matrix (including both mitochondrial and nuclear markers) had identical topologies, and although the result from the MP analysis was slightly less resolved, nodes were mostly congruent (Fig. 1; Supporting Information, Figs S1–S3). Basal outgroup relationships had low support and were somewhat different from the ones in the recent literature. In view of these

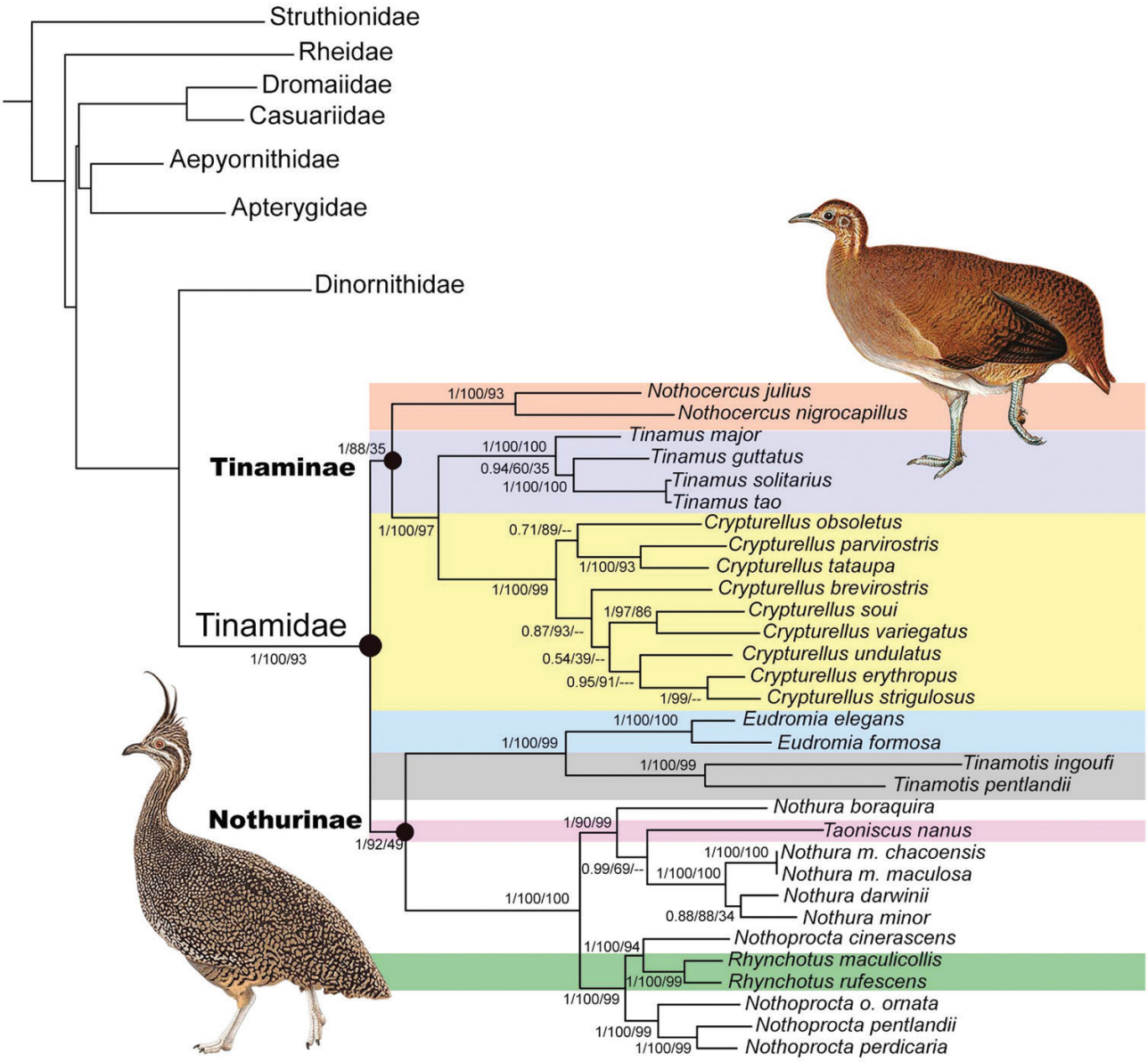


**Figure 1.** Bayesian inference (BI) majority consensus tree based on the concatenated molecular data, showing the phylogenetic relationships of tinamous (see also Supporting Information, Figs S6–S8). The maximum likelihood (ML) tree topology was identical to that of the BI tree. Clade-support values are indicated above branches (posterior probability under BI/bootstrap values under ML/bootstrap values under maximum parsimony, respectively).

results, we reran the analyses using a constraint to enforce the monophyly of the clade (Apteryigidae + Aepyornithidae) during tree search, following the groupings previously obtained by Mitchell *et al.* (2014) and Yonezawa *et al.* (2017). However, we found that outgroup relationships did not influence the ingroup tinamid topology (Fig. 1; Supporting Information, Figs S1–S3).

The analysis of the concatenated molecular data recovered the Tinamidae as a well-supported monophyletic group (Fig. 1), and the monophyly of most tinamou genera was also highly supported. Exceptions were *Nothoprocta*, which was paraphyletic owing to the inclusion of *Rhynchotus*, and *Nothura*, owing to the inclusion of *Taoniscus*. However, the latter relationship was not recovered in the MP searches, which showed a monophyletic *Nothura* instead.

All three methods (BI, ML and MP) subdivided Tinamidae into two well-supported groups: the forest-dwelling genera (*Crypturellus*, *Tinamus* and *Nothocercus*) and the open-area genera (*Taoniscus*, *Nothura*, *Nothoprocta*, *Tinamotis*, *Eudromia* and *Rhynchotus*) (Fig. 1; Supporting Information, Figs S3–S5). *Nothocercus* was the earliest diverging taxon of the forest-dwelling tinamous, with *Tinamus* and *Crypturellus* clustering together in all analyses. Within *Tinamus*, *Tinamus major* (Gmelin, 1789) and *Tinamus guttatus* (Pelzeln, 1863) were successive sister taxa to a well-supported clade (*Tinamus tao* + *Tinamus solitarius*). The relationships within the genus *Crypturellus* were fully resolved under BI and ML: the clade (*Crypturellus obsoletus* (Temminck, 1815) (*Crypturellus parvirostris* (Wagler, 1827) + *Crypturellus tataupa* (Temminck, 1815))) was recovered as sister to the other *Crypturellus* species. Next, *Crypturellus brevirostris* (Pelzeln, 1863) was sister to the remaining species of the genus. In turn, *Crypturellus soui* (Hermann, 1783) and *Crypturellus variegatus* (Gmelin, 1789) formed a group that was sister to the clade (*Crypturellus undulatus* (Temminck, 1815) + (*C. erythropus* + *Crypturellus strigulosus* (Temminck, 1815))). Under MP, relationships among *Crypturellus* species were less resolved, somewhat variable and lacking statistical support; the only supported relationships were between *C. parvirostris* and *C. tataupa* on the one hand and *C. soui* and *C. variegatus* on the other (Supporting Information, Fig. S3).

Within the open-area Nothurinae, *Tinamotis* and *Eudromia* grouped together in a clade that was sister to a group encompassing all remaining open-area genera. Within the latter, two suprageneric clades were recovered: (*Nothoprocta* + *Rhynchotus*) and (*Taoniscus* + *Nothura*). All these relationships received high statistical support. In both ML and BI analyses, *Nothura boraquira* (Spix, 1825) was sister to the remaining species, and *Taoniscus nanus* (Temminck, 1815), the dwarf tinamou, was sister to the well-supported sister clades of *Nothura maculosa maculosa* (Temminck, 1815) + *Nothura maculosa chacoensis* Conover, 1937 and *Nothura darwinii* Gray, 1867 + *Nothura minor* (Spix, 1825). The inclusion of *Taoniscus nanus* in *Nothura* was well supported in the BI and ML trees. In contrast, the MP analysis recovered the dwarf tinamou as sister to the suprageneric group consisting of (*Nothura* + (*Rhynchotus* + *Nothoprocta*)), although this arrangement lacked statistical support (see Fig. 1; Supporting Information, Fig. S3). The paraphyly of *Nothoprocta* owing to the inclusion of *Rhynchotus* was highly supported in all three analyses (Fig. 1; Supporting Information, Figs S3–S5). Within this clade, *Nothoprocta cinerascens* was sister to a monophyletic *Rhynchotus*, whereas the three other *Nothoprocta* species clustered together consistently, with high statistical support.

### Combined molecular and phenotypic trees

The combined analysis of molecular and phenotypic data allowed the inclusion of 18 tinamou species for which molecular data were not available. The trees recovered in this analysis were highly congruent and broadly resolved under both the traditional strategy and the EPA strategy (Fig. 2; Supporting Information, Figs S6–S9). A monophyletic family was again recovered with high support and subdivided into forest-dwelling (Tinaminae) and open-area (Nothurinae) clades as in the analyses based on molecular data alone. Differences between alternative trees were mainly for relationships showing lower support within *Crypturellus* and in the paraphyly of *Nothoprocta*, which was recovered under BI and ML, but not MP (Fig. 2; Supporting Information, Figs S6–S9). The strict consensus tree under MP (Supporting Information, Fig. S6) exhibited two polytomies involving some species of *Crypturellus* and *Nothoprocta*. In the case of *Nothoprocta*, the polytomy was caused by the unstable position of *Nothoprocta taczanowskii* (Sclater & Salvin, 1875), a taxon for which only morphological data were available. The a posteriori exclusion of this species from the MP consensus tree resulted in a reduced consensus tree mostly compatible with trees obtained with the other methods. In the latter trees, a clade including *Nothoprocta perdicaria* (Kittlitz, 1830), *Nothoprocta pentlandii* Gray, 1867 and *Nothoprocta curvirostris* (Sclater & Salvin, 1873) was recovered with medium to high support, but without internal resolution.

Within the forest dwelling Tinaminae, *Nothocercus* was well supported and, as in the molecular analysis, *Nothocercus julius* Bonaparte, 1854 was the sister taxon to the other two species [*Nothocercus bonapartei* (Gray,

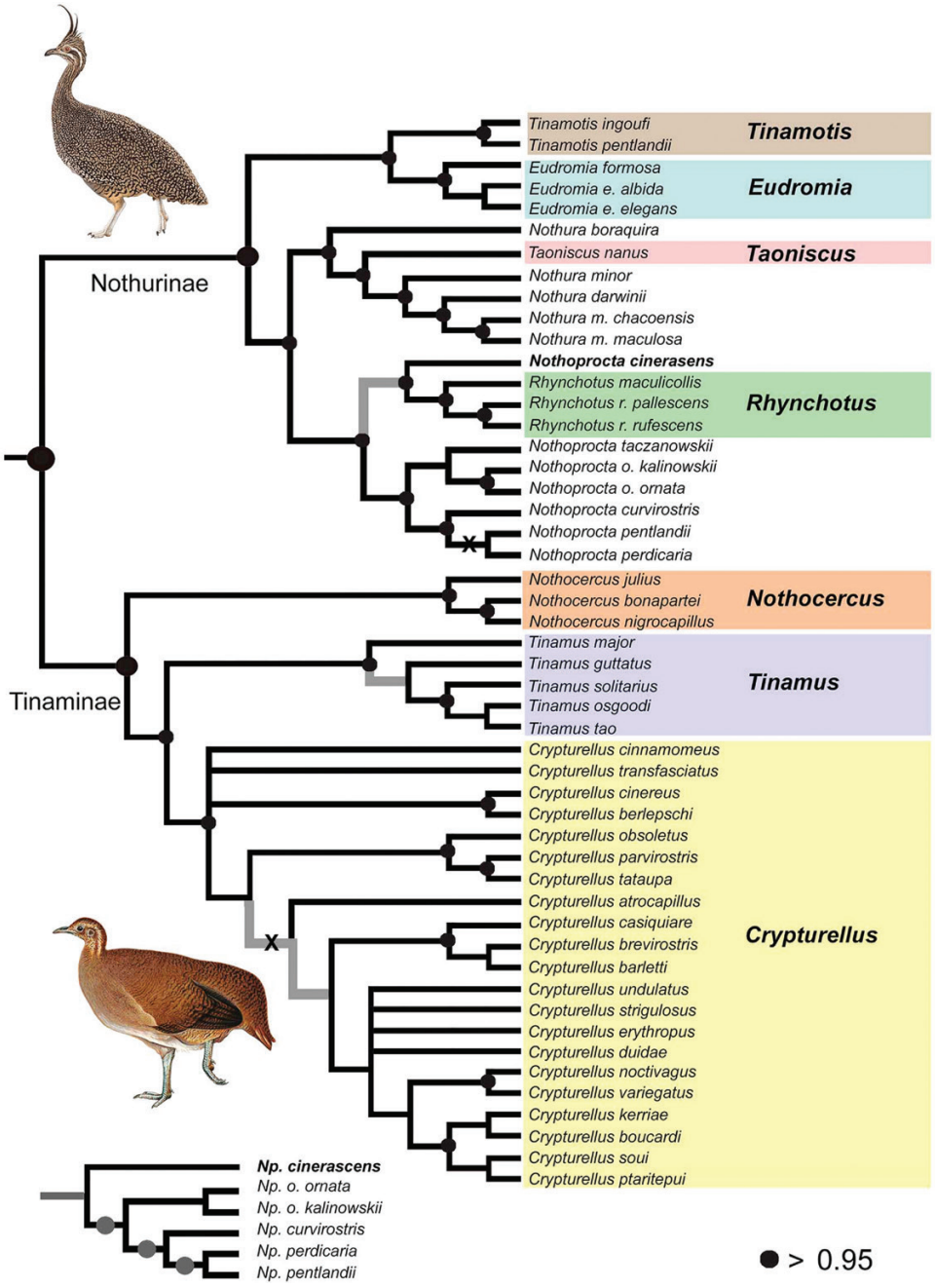


**Figure 2.** Relationships of the tinamous using a combined matrix of molecular and morphological data as inferred by Bayesian inference (BI) (Supporting Information, Fig. S7). The subtree topology in the inset was recovered under maximum parsimony (MP). Well-supported nodes having support values > 90% under MP and > 0.95 under BI are marked by dots on the cladogram. Differences among the BI topology and the topologies obtained with the MP (Supporting Information, Fig. S6) and maximum likelihood (ML) searches (Supporting Information, Fig. S8) are marked in grey and with an X, respectively.

1867) and *Nothocercus nigrocapillus* (Gray, 1867)]. Within *Tinamus*, *Tinamus guttatus* and *Tinamus major* clustered together in a clade sister to all other species, which formed a clade with high support in all analyses (Fig. 2; Supporting Information, Figs S6–S9). The largest tinamou clade, corresponding to the genus *Crypturellus*, was consistently recovered, but the relationships within the genus were less resolved than in the remaining polytypic genera. Thus, the combined evidence did not resolve the base of the *Crypturellus*

subtree (polytomy or poorly supported clades). However, some relationships within *Crypturellus* were consistently recovered with all search methods, usually with high support in the BI: [*Crypturellus cinereus* (Gmelin, 1789) + *Crypturellus berlepschi* Rothschild, 1897], [*C. obsoletus* + [*C. parvirostris* + *C. tataupa*]], [*Crypturellus casiquiare* Chapman, 1929 + [*C. brevirostris* + *Crypturellus barletti* (Sclater & Salvin, 1873)]], [*Crypturellus noctivagus* (Wied, 1820) + *C. variegatus*], [[*Crypturellus ptaritepui* Zimmer & Phelps, 1945 + *C. soui*] + [*Crypturellus boucardi* (Sclater, 1859) + *Crypturellus kerriae* (Chapman, 1915)]].

Within the open-area Nothurinae, the basal relationships were the same as in the molecular analysis. As expected, the samples that map onto subspecies of *Eudromia elegans* (Saint-Hilaire, 1832) (*Eudromia elegans albida* (Wetmore, 1921) + *Eudromia elegans elegans* Geoffroy Saint-Hilaire, 1832) were sisters to *Eudromia formosa* (Lillo, 1905), and *Taoniscus nanus* was again recovered within a paraphyletic *Nothura*. Within *Nothura*, we observed one of the few differences between the results from the molecular-only and the combined analyses: *Nothura darwinii* and *Nothura minor* appeared as sister taxa in the former, whereas in the combined analysis *Nothura darwinii* was sister to a highly supported and consistently recovered clade formed by (*Nothura m. maculosa* + *Nothura m. chacoensis*) (Fig. 2). *Rhynchotus* was recovered within *Nothoprocta* under ML and BI (as in the molecular analysis), but not under MP, although this arrangement had low support. However, the *Rhynchotus* clade was well supported across analyses, with *Rhynchotus maculicollis* (Gray, 1867) as the sister to the remaining species. As in the molecular analyses, the BI and ML recovered *Nothoprocta cinerascens* as sister to *Rhynchotus*, whereas the MP tree recovered *Nothoprocta cinerascens* as the sister taxon to all other species of *Nothoprocta*. The internal arrangement of *Nothoprocta* was inconsistent across methods. The BI and ML analyses recovered two clades of three taxa each: (*Nothoprocta taczanowskii* + [*Nothoprocta ornata kalinowskii* von Berlepsch & Stolzmann, 1901 + *Nothoprocta ornata ornata* (G. R. Gray, 1867)]) and (*Nothoprocta curvirostris* + *Nothoprocta pentlandii* + *Nothoprocta perdicaria*) (see Fig. 2, inset); in addition, the relationships within the latter subclade varied across methods (Supporting Information, Figs S6–S9).

### Fossil relationships

The unstable behaviour of some fragmentary fossil tinamous (Early Miocene MACN-SC-T and MACN-SC-H and the extinct species *Crypturellus reai* and *Nothura* sp.) observed by Bertelli *et al.* (2014) and in our own preliminary MP analysis was probably related to the limited information (i.e. missing data) and not attributable to conflicting scorings. After identifying these fossil terminals as responsible for topological instability, they were excluded a posteriori from the consensus MP tree and from the ML and BI analyses. Phylogenetic results including fossils showed marked differences across methods in topological resolution, again most probably attributable to the fragmentary scoring of fossil taxa (Supporting Information, Figs S10–S12).

Relationships of tinamid fossil taxa obtained in the ML analysis were the same as those recovered by Bertelli *et al.* (2014) using morphological characters only, confirming the phylogenetic placements of the oldest fossil fragments, MACN-SC-3610 and MACN-SC-3613, as sister to the genus *Crypturellus*. Also, they agreed in the systematic position of *E. olsoni*, the placement of *Eudromia* sp. as sister to the clade formed by the extant *Eudromia* and *Tinamotis*, and the position of the fossil taxon *Nothura parvula* (Brodkorb, 1963) as sister to a clade formed by the remaining open-area clades (*Nothura*, *Taoniscus*, *Rynchotus* and *Nothoprocta*). Our MP results showed less clade resolution, but similar results to the ML analysis (Supporting Information, Figs S10, S12). In contrast, the BI tree had little resolution in the ingroup, especially in the forest-dwelling clade (Supporting Information, Fig. S11). Interestingly, the position of *Lithornis* varied among analyses. In the ML and MP trees it was positioned as sister to Tinamidae, although without statistical support. In the BI tree it appeared as sister to all palaeognaths with 95% posterior probability.

### Character performance

The combined molecular and morphological analysis recovered a tree structure similar to the recently evaluated phylogeny by Bertelli (2017), and the distribution of synapomorphies from various character types (internal anatomy, external morphology, breeding, song structure, etc.) also showed a congruent hierarchical structure across analyses (see Supporting Information, Fig. S13). In the optimization of the current most parsimonious trees, phenotypic changes were distributed at almost every node of the ingroup subtree, with the exception of two clades within *Nothura* and *Crypturellus*. These intrageneric clades were not recovered by Bertelli (2017), although other nodes recovered only in the present study (e.g. relationships within *Nothoprocta* and *Tinamus*) did have synapomorphies provided by morphological and/or behavioural characters.

Internal anatomical characters (osteology and myology) were mainly diagnostic at higher hierarchical levels and were the primary source of synapomorphies for Tinamidae. This result was related to the fact that external morphological and behavioural characters were mostly (with the exception of a few breeding, leg and bill characters) non-comparable between Tinamidae and the ratites. Nevertheless, these character types provided unambiguous synapomorphies for almost all clades of the tinamou subtree. In fact, breeding and external morphology characters have been determinant in some areas of the tree, exclusively providing synapomorphies for 17 of the 43 ingroup nodes, thus confirming their value as a source of phylogenetic information. It should also be noted that some integumentary characters traditionally used in bird systematics (e.g. colour variations) have been less informative, requiring many extra steps under current optimal topologies. Mapping of feather patterns, osteology and egg coloration is shown in Figure 4.

### Divergence age estimations

The divergence-date estimates differed between the two calibration schemes used and depending on the matrix used (Fig. 3; Supporting Information, Figs S14–S17). The scheme that considered *Lithornis* as sister to Tinamidae recovered older ages in general. In contrast, divergence dates were notably more recent when estimates were based on *RAG2* sequences only. Thus, when considering *Lithornis* as the sister group, crown Tinamidae was dated at 47.2 Myr old with the complete matrix and 37.8 Myr old with the *RAG2* matrix. When lithornids were excluded from the calibration and the *Diogenornis* constraint was applied, crown Tinamidae was estimated to be 40.1 or 31 Myr old, with the complete and *RAG2*-only matrices, respectively. All other clade divergence ages estimated within Tinamidae followed the same pattern, becoming more recent in the calibration scheme that excluded lithornithids.

## DISCUSSION

Tinamous are of particular importance in our efforts to understand both the biology of modern birds and the shape of their evolutionary tree. Recent genome-level research that has included selected tinamou species has illustrated their importance, and comparisons of ratites and tinamous have provided important new insights on the evolution and possible duplications of their mitogenomes (Urantówka *et al.*, 2020) and on the influence of regulatory evolution on morphological convergence in ratites, such as loss of flight (Sackton *et al.*, 2019). The lack of a detailed phylogeny for the family has hindered efforts to delve further into the evolution of the group. Here, we present the first detailed phylogenetic analysis and divergence-date estimation including a significant number of tinamou species both extant and fossil.

### Morphological and molecular evidence

The molecular analysis recovered a tree structure highly congruent to those of trees based solely on phenotypic data (results not shown; Bertelli *et al.*, 2014; Bertelli, 2017), thus firmly confirming the backbone structure for the phylogeny of the family (Fig. 1). The total-evidence analysis corroborated the hypothesis of two major groups within tinamous: the open-area Nothurinae ((*Tinamotis* + *Eudromia*) + ((*Taoniscus* +*Nothura*) + (*Nothoprocta* + *Rhynchotus*))) and the forest-dwelling Tinaminae (*Nothocercus* + (*Tinamus* + *Crypturellus*)) (Fig. 2). Moreover, datasets were also congruent in supporting some suprageneric groups, the monophyly of polytypic genera (except for *Nothoprocta* and *Nothura*) and groups nested within genera. This congruence across independent data sources provides further support for the phylogenetic hypothesis presented herein, allowing for a systematic classification based on robust phylogenetic evidence, supported by phenotypic synapomorphies and the study of character evolution.

Within the Nothurinae, in particular, results were highly congruent across datasets and methods, and the relationships remained basically the same as the ones recovered in previous morphological studies (Bertelli *et al.*, 2014; Bertelli, 2017). Among those highly supported and congruent relationships were the monophyly of *Tinamotis* and *Eudromia* and their sister relationship. As expected, the subspecies of *E. elegans* (*E. e. albida* + *E. e. elegans*) were sisters to *E. formosa*, relationships consistently supported across different types of evidence (Bertelli *et al.*, 2014; Bertelli, 2017). *Taoniscus nanus* was recovered within a paraphyletic *Nothura* in most analyses, except for the molecular-only MP tree (Bertelli *et al.*, 2014; Bertelli, 2017). However, the specific phylogenetic position of *Taoniscus nanus* was generally conflictive and had low support across datasets and methods; the exceptions were the BI trees, which supported a paraphyletic *Nothura*, with *Taoniscus* as sister to a clade formed by all *Nothura* species but *Nothura boraquira*. The conflict and lack of support could be attributable to the large amount of missing data for this species in the molecular matrix (Supporting Information, Table S1), because only sequences of the mitochondrial genes *Cytb* and *ND2* could be obtained for this study. Our results, together with those presented by Bertelli (2017), point to a taxonomic problem in need of further

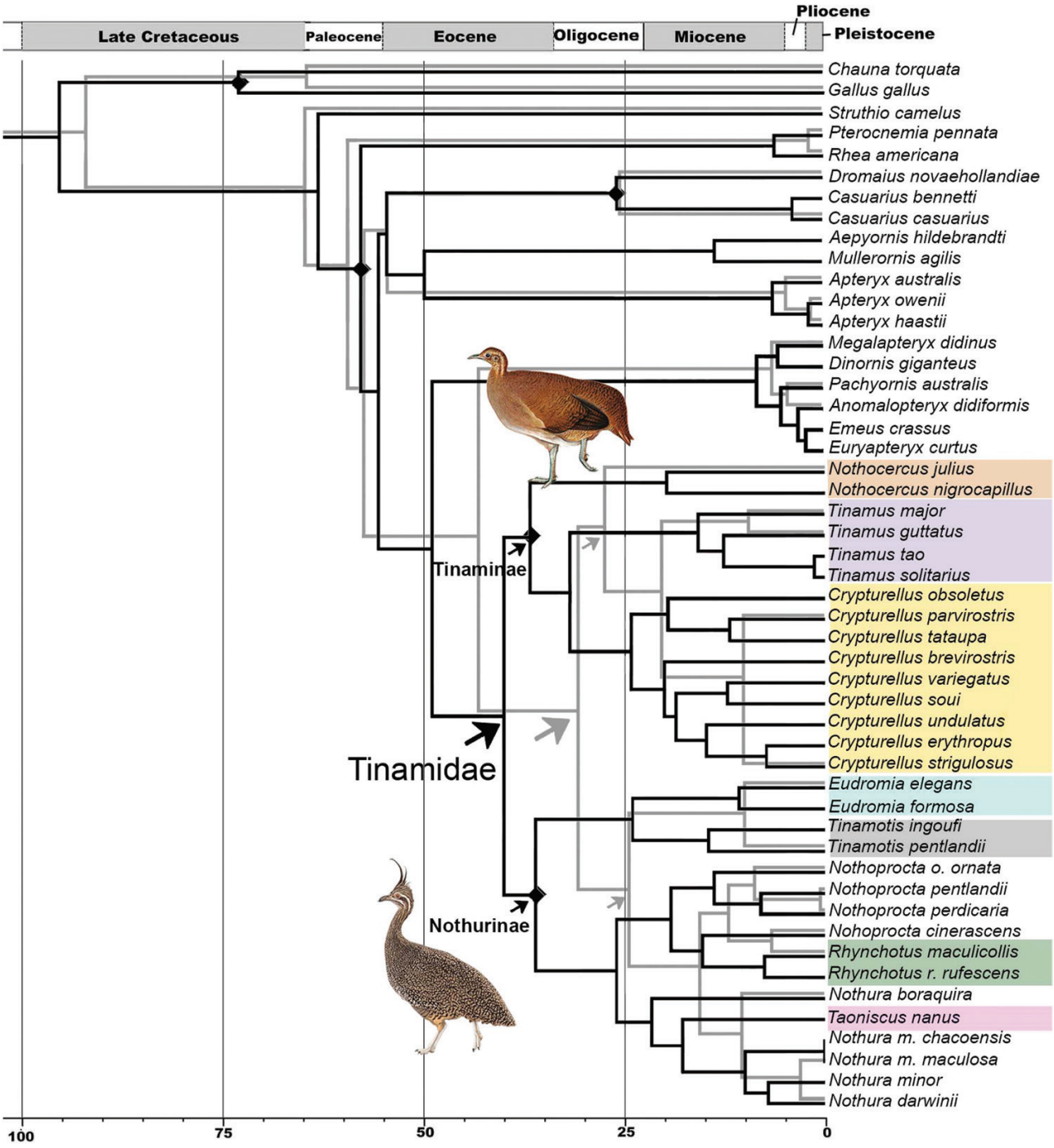


**Figure 3.** Divergence-date estimates obtained with the two alternative molecular matrices (black lines, complete; grey lines, *RAG2* only). In both cases, the fossil-based calibration scheme used the *Diogenornis* age constraint (see Table 1). Nodes used in fossil calibration are marked with diamonds.

investigation, ideally with more molecular data for *Taoniscus nanus*.

The main exception to a general agreement across different data sources involved relationships within *Nothoprocta*, with the molecular data challenging previous phenotypic results that recovered a strongly supported, monophyletic *Nothoprocta* (Bertelli *et al.*, 2014; Bertelli, 2017). Our analyses also found a strong signal for a sister relationship between *Nothoprocta cinerascens* and the genus *Rhynchotus*.

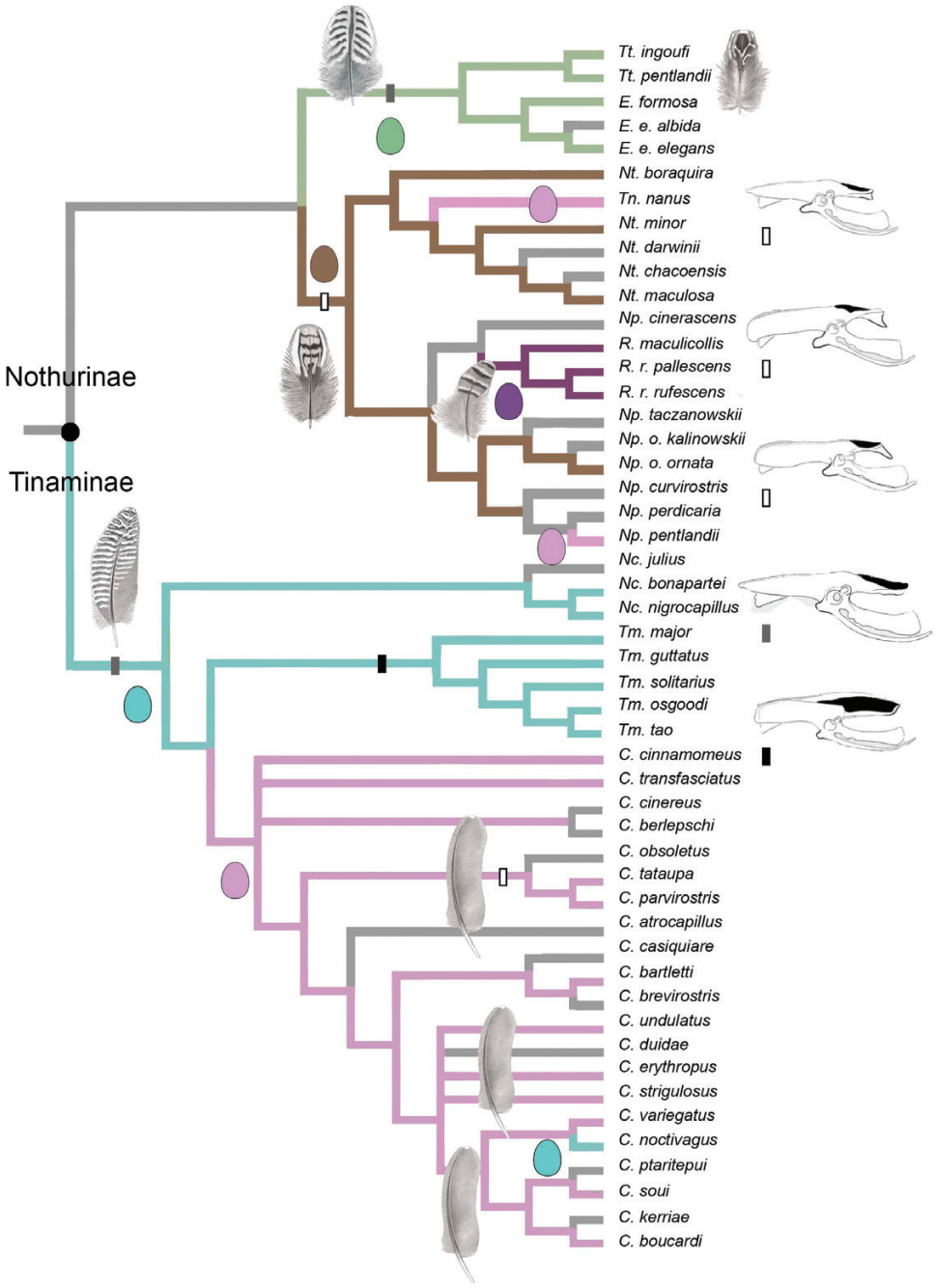


**Figure 4.** Taxonomic distribution and optimization of phenotypic characters: eggshell coloration, development of postacetabular pelvis and changes in plumage pattern (characters 9, 101 and 185, described in more detail in the Supporting Information, Appendix S1). For the data matrix, see the Supporting Information (Appendix S2). Further discussion is provided in the main text.

In our total-evidence analysis, the latter result was maintained (except under MP, but with low support); the molecular data dominated over the phenotypic data in supporting the paraphyly of *Nothoprocta* (Fig. 2). The relationship between *Nothoprocta cinerascens* and *Rhynchotus* recovered by the molecular data was supported by a single morphological character, colour of mandible (character 172), an integumentary character that has been shown to be less informative than other morphological characters. However, the monophyly of the genus *Rhynchotus* was well supported across analyses. As expected, *Rhynchotus rufescens rufescens*

(Temminck, 1815) and *Rhynchotus rufescens pallescens* (Kothe, 1907) formed a clade that was recovered consistently across datasets and methods (Bertelli *et al.*, 2014; Bertelli, 2017). Within the genus *Nothoprocta*, a clade consisting of (*Nothoprocta taczanowskii* (*Nothoprocta o. ornata* + *Nothoprocta o. kalinowskii*)) received high support in the combined analyses, although this arrangement differed from previous morphological results (Bertelli, 2017). Relationships among the remaining *Nothoprocta* species (*Nothoprocta curvirostris*, *Nothoprocta pentlandii* and *Nothoprocta perdicaria*) were inconsistent across both datasets and phylogenetic methods. This result could be explained by the lack of molecular data for *Nothoprocta curvirostris*, combined with a lack of phylogenetic signal for the relationship of *Nothoprocta pentlandii* based on phenotypic data alone (Bertelli, 2017).

Among the forest-dwelling tinamous, *Nothocercus* was resolved as sister to the other taxa (Figs 1, 2; Bertelli *et al.*, 2017). The relationships among *Nothocercus* species were also highly congruent across datasets and methods, with *Nothocercus bonapartei* and *Nothocercus nigrocapillius* appearing as sister species with high support. In contrast, the relationships within *Tinamus* disagreed with the ones obtained previously in a phenotypic analysis (Bertelli *et al.*, 2017), although this difference could be explained by a different 'rooting' of the genus. Within *Crypturellus*, most nodes were incongruent across analyses and/or had low statistical support. However, a few clades were recovered consistently, and four of those were supported statistically (Fig. 2; Bertelli *et al.*, 2014; Bertelli, 2017). *Crypturellus*, the most diverse genus of Tinamidae, is also the genus with the sparsest sampling in the molecular matrix, with only ~35% of its diversity included in our analyses. Moreover, among the nine *Crypturellus* species in the molecular matrix, five (*C. brevirostris*, *C. cinereus*, *C. erythropus*, *C. obsoletus* and *C. strigulosus*) are represented by only one mitochondrial gene. Therefore, for a better understanding of relationships within *Crypturellus* it will be necessary to carry out further analyses with a more complete molecular matrix for the genus. Although our present dataset contains some initial results for samples from populations that correspond to named subspecies, we consider results at the subspecific level to be preliminary and not sufficiently robust at this point to support taxonomic revisions. This and other questions of species delimitation will be explored in a separate study with additional population-level data and a wider geographical sampling. An in-depth discussion of character evolution and implications for taxonomic classification within the family is under development for separate publication.

### Tempo of diversification in tinamous

Several recent publications have addressed the timing of bird diversification. Although these publications did include tinamids, these were never represented by more than four species (Mitchell *et al.*, 2014; Claramunt & Cracraft, 2015; Prum *et al.*, 2015; Yonezawa *et al.*, 2017; Kimball *et al.*, 2019). Moreover, tinamid fossils were rarely used in calibrations (except for Claramunt & Cracraft, 2015, who included one tinamid calibration point). Thus, this is the first study that includes both a large sample of tinamou species and internal calibrations for the group. Here, we obtained four different estimates based on different calibration schemes and matrices (Fig. 3; Table 2). This variation and dependence on the particular dataset have been observed by other authors (Table 2; Mitchell *et al.*, 2014). Our results show that assuming that lithornids are sister to tinamids produces older ages irrespective of the dataset used. It is clear that determining the exact phylogenetic position of lithornids will be important for understanding the timing of palaeognath diversification. The extinct lithornithids, such as *Lithornis*, were volant palaeognath birds reported from the late Palaeocene to middle Eocene of North America and Europe (Mayr, 2009). Recently, Nesbitt & Clarke (2016) reviewed the relationships of lithornids and concluded that their apparent close relationship

**Table 2.** Comparison of divergence dates across studies (in millions of years ago)

| Dating source | Galloanserae | Palaeoganthae | Stem Tinamidae | Crown Tinamidae |
|---|---|---|---|---|
| (*Lithornis* + Tinamidae) complete matrix | 73.2 (64.3–83.3) | 73.4 (64.0–85.1) | 57.5 (55.2–63.4) | 47.2 (39.9–53.7) |
| *Diogenornis* complete matrix | 73.2 (63.4–82.3) | 63.2 (57.3–72.5) | 49.1 (42.2–56.4) | 40.1 (29.6–43.0) |
| (*Lithornis* + Tinamidae) *RAG2* | 66.6 (49.9–83.9) | 85.11 (67.6–109.1) | 58.9 (55.4–66.7) | 41.1 (29.7–52.1) |
| *Diogenornis RAG2* | 65.2 (45.6–81.7) | 65.9 (56.8–82.2) | 43.7 (32.8–54.4) | 31.7 (23.6–40.6) |
| Mitchell *et al.* (2014) (mitochondrial) | 73 | 63.3 (52.3–74.8) | 58.0 (49.5–68.1) | 41.9 (34.2–50.7) |
| Mitchell *et al.* (2014) (nuclear) | – | 69.4 (56.6–83.3) | 62.3 (49.8–75.9) | 36.8 (27.5–47.4) |
| Prum *et al.* (2015) | ~73 (68–80) | ~54 (40–69) | – | ~25 (12–36) |
| Claramunt & Cracraft (2015) | 72.5 | 65.3 (~57–74) | – | ~30 (19–42) |
| Yonezawa *et al.* (2017) | 75.3 | 79.58 | 53.32 (46–63) | ~30 (25–34) |

to tinamids is attributable to parallel retention of plesiomorphic characters and that lithornithids are most probably sister to all palaeognaths. This result was later corroborated by Yonezawa *et al.* (2017) using a dataset combining molecular data and a set of non-homoplasious morphological characters. Some of our results, namely our BI tree, support these recent studies, recovering *Lithornis* as sister of Palaeognathae; the alternative phylogenetic position of *Lithornis* as sister to tinamous was recovered in our MP and ML trees, although without statistical support (Supporting Information, Figs S8–S10).

Another well-preserved, ancient flightless palaeognath fossil taxon is *Diogenornis fragilis* from the early Eocene (55 Mya) of Brazil (Alvarenga, 1983). Although *Diogenornis* was never included in a phylogenetic study, shared morphological apomorphies strongly suggest that this fossil is related to the extant Rheidae. In our analyses, dating schemes using this fossil to calibrate the palaeognath diversification resulted in younger age estimates for the group (~63–66 Mya). This range places the origin of extant paleognaths around the Cretaceous–Palaeogene (KPg) boundary and is similar to the estimates obtained by Claramunt & Cracraft (2015) in a detailed study of divergence dates in birds that included a large number of fossil calibration points; however, other authors estimated older ages for the group (Table 2). Molecular clock calibrations using *Diogenornis* place the origin of the extant tinamous in the late Eocene (complete matrix) or early Oligocene (*RAG2* matrix).

Although only fragmentary fossil tinamous have been preserved, some diagnostic features of postcranial elements (remains of the coracoids, humeri, tibiotarsi and tarsometatarsi) are shared with living species, including derived character states supporting their position within the family (Bertelli *et al.*, 2014). In fact, even the oldest fossils are similar to extant taxa, and some could be identified readily at genus level despite being fragmentary (e.g. *Crypturellus reai*). In agreement with that, our estimates suggest that crown Tinamidae is much older (31–40 Mya) than the oldest tinamid fossils (from the early middle Miocene). It is also notable that the internal nodes of Tinamidae are much older than those of the other palaeognath families, although it could be related to the low species diversity in the latter groups. Apart from Tinamidae, the oldest family crown age is that of Casuariidae, estimated at ~26 Mya.

It is not clear how the exceptional substitution rates of tinamids could bias their age estimates (Haddrath & Baker, 2001; Porzecanski, 2003; Mitchell *et al.*, 2014; Yonezawa *et al.*, 2017). Our complete dataset included mostly fast-evolving loci (mitochondrial loci and nuclear introns) and recovered older dates than the ones obtained from sequences of *RAG2*, which is a conserved protein-coding gene. To gain a better understanding of the tempo of diversification within tinamous, it will be crucial to include more complete sampling of slowly evolving nuclear loci in future studies. The estimated ages of crown tinamous obtained with *RAG2* and with the *Diogenornis* calibration were similar to those obtained by Claramunt & Cracraft (2015) and Yonezawa *et al.* (2017), placing the crown age of the group in the early Oligocene (Table 2). The former study was based on slowly evolving nuclear loci and the latter on a large genomic dataset, but using different taxon sampling and different fossil calibration. Prum *et al.* (2015) obtained even more recent estimates (25 Mya), which were discussed by Yonezawa *et al.* (2017) as an artefact of the sparse palaeognath taxon sampling and the calibration used. In contrast, our complete matrix recovered ages more similar to those obtained by Mitchell *et al.* (2014) using mitochondrial genes (Table 2).

According to our dating analyses, tinamids started to diversify between the late Eocene and early Oligocene, coinciding with a lowering of the temperature and the appearance of open-area environments in South America, which caused a major faunal turnover (Woodburne *et al.*, 2014; Dunn *et al.*, 2015). At this time, the first split in the group gave rise to the open-area subfamily Nothurinae and the forested-area Tinaminae. About 4 Myr after this first cladogenetic event, it appears that the two subfamilies started to diversify almost simultaneously. If tinamous originated in the Eocene, we could argue that their ancestral habitat was the subtropical forest that characterized the palaeoenviromental conditions of this period. Coincidentally, the earliest known tinamou fossils were likely to be forest dwellers. They were formed ~16.5 Mya in a coastal area in southern Argentina; these remains (MACN-SC-3610 and MACN-SC-3613) and other early-mid Miocene fossils (e.g. *Crypturellus reai*; Bertelli *et al.*, 2014) were placed among the forest-dwelling Tinaminae. These placements are in accordance with the palaeoenvironmental conditions of Patagonia in the early–middle Miocene, which have been characterized as a humid subtropical, forested landscape transitioning into the open-area environments that characterize most of the region today (Vizcaíno *et al.*, 2012). Currently, forest-dwelling tinamous have a mid-northern distribution in South America, whereas nothurine species are widespread in the south. This would be consistent with their distributions shifting over time as landscapes changed and as southern and central South America became more arid.

### Insights into tinamou evolution

The phylogenetic results imply an early divergence between forest and open-area taxa followed by little

plasticity in broad habitat preferences over the rest of the evolution of the group. Tinamou congeners are found to share the same broad habitat preferences, confirming previous findings of group specificity in this matter, with the only exception being the species *C. parvirostris* and *C. tataupa*, which, despite belonging to a large clade of forest taxa, are mainly found in arid or open areas, such as grasslands and dry forests. However, in each subfamily a recurrent pattern can be observed, whereby a single lineage displays markedly more diversification (*Crypturellus* and *Nothura* + its closest relatives, respectively) than its sister lineages, which display restricted diversification, even over substantial evolutionary time.

Our analysis dated the origin of Nothurinae (open-area tinamous) right before or at the origin of woodland savannas in South America (in latest Eocene–earliest Oligocene) (Dunn *et al.*, 2015). One possible scenario is that Tinaminae remained in the ancestral, forested habitat of the tinamids, whereas the ancestor of Nothurinae colonized the open areas. This habitat switch probably involved a series of phenotypic modifications to an entirely new environment in the open-area group. For instance, the reconstruction of evolutionary changes of plumage characters suggests that the rather simple plumage design of the forest tinamous was replaced by more complex patterns with distinctive plumage variations in the open-area species (Fig. 4). These differences in plumage have been hypothesized to be adaptive and related to camouflage advantages in different habitat types (Sick, 1984; Cabot, 1992; Davies, 2002). Osteological modifications probably related to flight or terrestrial locomotion were also observed in the open-area groups (a more detailed discussion on the optimization of these and other morphological characters is provided by Bertelli *et al.*, 2014; Fig. 4). Tinamous are mainly terrestrial birds; however, most open-area species have short flights alternating between gliding periods (Fjeldså & Krabbe, 1990). This enhanced flight capability in Nothurinae is correlated with marked changes in the pectoral girdle (sternum and coracoids). Likewise, the development and notable changes of the postacetabular pelvis (main area of origin of muscles that insert on the distal femur and proximal tibiotarsus) of the open-area groups could be related to differences in the cursorial ability and running patterns of tinamous (Hudson *et al.*, 1972). Other osteological differences between the two main tinamou groups were observed in cranial structures, such as the lacrimal–ectethmoid plate, mandibular articular areas and the quadrate, which are conspicuously developed in the open-area groups and are likely to be related to feeding adaptations (Elzanowski, 1987). Future studies on the functional correlates of these character transformations will advance our understanding of the evolution of anatomical structures of tinamous.

The phylogenetic hypotheses presented herein also provided insights into the evolution of egg pigmentation. With the inclusion of moas (which may have either white or green eggs) in the analysis, the optimization of the ancestral state was ambiguous (Fig. 4). In the open-area groups, two main types of changes were optimized: the cyaninic green of *Tinamotis* + *Eudromia* and the mostly porphyrinic colours (brownish, chocolate or purple) of the remaining steppe tinamous. Within the forest-dwelling group, the basic eggshell colorations were the cyaninic blues, and the main trend in eggshell pigmentation was the transformation from cyaninic bluish to pinkish-violet colours in *Crypturellus* (reversed in *C. noctivagus*) (Fig. 4). Despite this unique and interesting pattern, little is known about the function of eggshell coloration in tinamous. Previous studies suggest that egg coloration might be related to communal nesting, although there is no compelling evidence of such behaviour in tinamous (Hanley *et al.*, 2013). Alternative hypotheses include a visual cue of nest location (Brennan, 2010). We suggest that camouflage should not be ruled out, because there seems to be a general correlation with habitat type, but additional *in situ* studies are necessary to test this and other hypotheses.

## Conclusions

The present analysis of combined evidence strengthens previous morphological studies (Bertelli *et al.*, 2014; Bertelli, 2017), clarifies the higher-level relationships within Tinamidae and confirms the backbone structure of the tinamou tree and a classification based on it (subfamilies, suprageneric relationships and most genera). Most incongruent nodes across our main analyses were restricted to groups with relatively low support (e.g. some areas of the *Crypturellus* subtree) and alternative results might not be attributable to real conflict, but to a lack of phylogenetic signal. Only the position of two terminals, *Nothoprocta cinerascens* and *Taoniscus nanus*, might alter the current understanding of genera requiring systematic changes. A more complete molecular matrix, in terms of both taxon and data sampling, would improve the resolution of these relationships and allow for taxonomic revisions based on more robust evidence. Likewise, data on more conserved loci might improve molecular dating of their time of origin, because age estimates of tinamou divergence are unstable and depend on the loci used. Our results placed the origin of

crown tinamids between the late Eocene and early Oligocene.

Climatic and vegetational changes, organismal ecology and morphological evolution are all likely to have played a role in shaping the diverse phenotypes found in tinamous. This has resulted in a bird family that is distinctive and successful in all the major biomes in South America. As the evolution of this unique bird family comes into sharper focus, it will continue to illuminate the earliest diversification events in avian evolution and the speciation mechanisms that shape continental biotas.

## ACKNOWLEDGEMENTS

F.C.A. and S.B.B. contributed equally to this work. This paper includes results from the doctoral research by A.L.P. at Columbia University, which received generous support from the American Museum of Natural History's Center for Biodiversity and Conservation through its International Graduate Student Fellowship Program and the Department of Ornithology through the Frank M. Chapman Memorial Fund and the Cullman Research Facility. We are grateful to the curators and collection managers who kindly provided access to their collections, collection data, tissue and/or skin samples for this study, without which this project would not have been possible. We give special thanks to Enrique Guanuco (Fundación Miguel Lillo) for tinamou illustrations. We thank Liliana Dávalos, Marcos Mirande and two anonymous reviewers for useful comments that helped to improve the manuscript. Different stages of the research were supported by Consejo Nacional de Investigaciones Científicas y Tecnológicas (PIP2015-2017 to S.B.B. and F.C.A.), Fondo para la Invetigación Científica y Tecnológica (PICT-2015-2009 and PICT 2019-04211 to S.B.B. and F.C.A.), the American Museum of Natural History (Collection Study Grant) to S.B.B., and National Science Foundation and National Aeronautics and Space Administration (grant 1241066) to J.L.C. The authors declare that they have no conflict of interest.

## REFERENCES

**Alvarenga HMF. 1983.** Uma ave ratitae do Paleoceno Brasileiro: bacia calcária de Itaboraí, Estado do Rio de Janeiro, Brasil. *Boletim do Museu Nacional, Nova Série, Geologia* **41:** 1–8.

**Berger SA**, **Krompass D**, **Stamatakis A. 2011.** Performance, accuracy, and Web server for evolutionary placement of short sequence reads under maximum likelihood. *Systematic Biology* **60:** 291–302.

**Bertelli S. 2017.** Advances on tinamou phylogeny: an assembled cladistic study of the volant palaeognathous birds. *Cladistics* **33:** 351–374.

**Bertelli S**, **Chiappe LM. 2005.** Earliest tinamous (Aves: Palaeognathae) from the Miocene of Argentina and their phylogenetic position. *Contributions in Science* **502:** 1–20.

**Bertelli S**, **Chiappe LM**, **Mayr G. 2014.** Phylogenetic interrelationships of living and extinct Tinamidae, flying palaeognathous birds from the New World. *Zoological Journal of the Linnean Society* **172:** 145–184.

**Bertelli S**, **Giannini NP. 2013.** On the use of intergumentary characters in bird phylogeny: the case of *Tinamus osgoodi* (Palaeognathae: Tinamidae) and plumage character coding. *Acta Zoologica Lilloana* **57:** 57–71.

**Bertelli S**, **Giannini NP**, **Goloboff PA. 2002.** A phylogeny of the tinamous (Aves: Palaeognathiformes) based on integumentary characters. *Systematic Biology* **51:** 959–979.

**Bertelli S**, **Tubaro P. 2002.** Body mass and habitat correlates of song structure in a primitive group of birds. *Biological Journal of the Linnean Society* **77:** 423–430.

**Bertelli S, Porzecanski AL. 2004.** Tinamou (Tinamidae) systematics: a preliminary combined analysis of morphology and molecules. *Ornitologia Neotropical* **15:** 293–299.

**Bouckaert R**, **Heled J**, **Kühnert D**, **Vaughan T**, **Wu CH**, **Xie D. 2014.** BEAST 2: a software platform for Bayesian evolutionary analysis. *PLoS Computational Biology* **10:** e1003537.

**Bourdon EA**, **Ricqlés DE**, **Cubo J. 2009.** A new transantarctic relationship: morphological evidence for a Rheidae–Dromaiidae–Casuariidae clade (Aves, Palaeognathae, Ratitae). *Zoological Journal of the Linnean Society* **156:** 641–663.

**Brennan PL. 2010.** Clutch predation in great tinamous *Tinamus major* and implications for the evolution of egg color. *Journal of Avian Biology* **41:** 419–426.

**Cabot J. 1992.** Order tinamiformes. In: del Hoyo J, Elliot A, Sargatal J, eds. *Handbook of the birds of the world, vol. 1. Ostrich to ducks*. Barcelona: Lynx Edicions, 112–138.

**Claramunt S**, **Cracraft J. 2015.** A new time reveals Earth history's imprint on the evolution of modern birds. *Science Advances* **1:** e1501005.

**Cloutier A**, **Sackton TB**, **Grayson P**, **Clamp M**, **Baker AJ**, **Edwards SW. 2019.** Whole-genome analyses resolve the phylogeny of flightless birds (Palaeognathae) in the presence of an empirical anomaly zone. *Systematic Biology* **68:** 937–955.

**Cracraft JL. 1974.** Phylogeny and evolution of the ratite birds. *Ibis* **116:** 494–521.

**Cracraft JL**, **Feinstein J**, **Vaughn J**, **Helm-Bychowski K. 1998.** Sorting out tigers (*Panthera tigris*): mitochondrial sequences, nuclear inserts, systematics, and conservation genetics. *Animal Conservation Forum* **1:** 139–150.

**Davies SJJF. 2002.** *Ratites and tinamous. Tinamidae, Rheidae, Dromaiidae, Casuariidae, Apterygidae, Struthionidae*. New York: Oxford University Press.

**Dunn R**, **Stromberg C**, **Madden RH**, **Kohn MJ. 2015.** Linked canopy, climate, and faunal change in Cenozoic of Patagonia. *Science* **347:** 248–261.

**Elzanowski A. 1987.** Cranial and eyelid muscles and ligaments of the tinamous (Aves: Tinamiformes). *Zoologische Jahrbücher: Abteilung für Anatomie und Ontogenie der Tiere* **116:** 63–118.

**Fjeldså J**, **Krabbe N. 1990.** *Birds of the high Andes*. Copenhagen Zoological Museum: Museum Danmark.

**Goloboff PA, Farris JS, Nixon KC. 2008.** TNT, a free program for phylogenetic analysis. *Cladistics* **24:** 774–786.

**Hackett SJ. 1996.** Molecular phylogenetics and biogeography of tanagers in the genus *Ramphocelus* (Aves). *Molecular Phylogenetics and Evolution* **5:** 368–382.

**Hackett SJ, Kimball RT, Reddy S, Bowie RCK, Braun EL, Braun MJ, Chojnowski JL, Cox WA, Han KL, Harshman J, Huddleston CJ, Marks BD, Miglia KJ, Moore WS, Sheldon FH, Steadman DW, Witt C, Yuri T. 2008.** A phylogenomic study of birds reveals their evolutionary history. *Science* **320:** 1763–1768.

**Haddrath O, Baker AJ. 2001.** Complete mitochondrial DNA genome sequences of extinct birds: ratite phylogenetics and the vicariance biogeography hypothesis. *Proceedings of the Royal Society B: Biological Science* **268:** 939–945.

**Haddrath O, Baker AJ. 2012.** Multiple nuclear genes and retroposons support vicariance and dispersal of the palaeognaths, and an Early Cretaceous origin of modern birds. *Proceedings of the Royal Society B: Biological Science* **279:** 4617–4625.

**Hanley D, Stoddard MC, Cassey P, Brennan PL. 2013.** Eggshell conspicuousness in ground nesting birds: do conspicuous eggshells signal nest location to conspecifics? *Avian Biology Research* **6:** 147–156.

**Harshman J, Braun EL, Braun ML, Huddleston CJ, Bowie RCK, Chojnowski, JL, Hackett SJ, Han KL, Kimball RT, Marks BD, Miglia KJ, Moore WS, Reddy S, Sheldon FH, Steadman DW, Steppan SJ, Witt CC, Yuri T. 2008.** Phylogenomic evidence for multiple losses of flight in ratite birds. *Proceedings of the National Academy of Sciences of the USA* **105:** 13462–13467.

**Houde PW. 1988**. *Paleognathous birds from the early Tertiary of the Northern Hemisphere*. Cambridge: Publications of the Nuttall Ornithological Club.

**Hudson GE, Schreiweis DO, Wang SYC, Lancaster DA. 1972.** A numerical study of the wing and leg muscles of tinamous (Tinamidae). *Northwest Science* **46:** 207–255.

**Jarvis ED, Mirarab S, Aberer AJ, Li B, Houde P, Li C, Ho SYW, Faircloth BC, Nabholz B, Howard JT, Suh A, Weber CC, da Fonseca RR, Li H, Zhang F, Li H, Zhou L, Narula N, Liu L, Ganapathy G, Boussau B, Bayzid S, Zavidovych V, Subramanian S, Gabaldon T, Capella-Gutierrez S, Huerta-Cepas J, Rekepalli B, Munch K, Schierup M, Lindow B, Warren BC, Ray D, Green RE, Bruford MW, Zhan X, Dixon A, Li S, Li N, Huang Y, Derryberry EP, Frost Bertelsen M, Sheldon FH, Brumfield RT, Mello CV, Lovell PV, Mirthlin M, Cruz Schneider MP, Prosdocimi F, Samaniego JA, Vargas Velazquez AM, Alfaro-Nunez A, Campos PF, Petersen B, Sicheritz-Ponten T, Pas A, Bailey T, Scofield P, Bunce M, Lambert DM, Zhou Q, Perelman P, Driskell AC, Shapiro B, Xiong Z, Zeng Y, Liu S, Li Z, Liu B, Wu K, Xiao J, Yinqi X, Zhen, Q, Zhang Y, Yang H, Wang J, Smeds L, Rheindt FE, Braun F, Fjeldsa J, Orlando L, Barker FK, Jønsson KA, Johnson W, Koepfli KP, O'Brien S, Haussler D, Ryder OA, Carsten R, Willerslev E, Graves GR, Glen TC, McCormack J, Burt D, Ellegren H, Alstrom P, Edwards SV, Stamatakis A, Mindell DP, Cracraft J, Braun EL, Warnow T, Jun W, Gilbert MP, Zhang G. 2014.** Whole-genome analyses resolve early branches in the tree of life of modern birds. *Science* **346:** 1320–1331.

**Katoh K, Standley DM. 2013.** MAFFT multiple sequence alignment software version 7: improvements in performance and usability. *Molecular Biology and Evolution* **30:** 772–780.

**Kimball RT, Oliveros CH, Wang N, White ND, Barker FK, Field DF, Ksepka DT. 2019.** A phylogenomic supertree of birds. *Diversity* **11:** 109.

**Lanfear R, Calcott B, Ho SYW, Guindon S. 2012.** PartitionFinder: combined selection of partitioning schemes and substitution models for phylogenetic analyses. *Molecular Biology and Evolution* **29:** 1695–1701.

**Lee K, Feinstein J, Cracraft, JL. 1997.** The phylogeny of ratite birds: resolving conflicts between molecular and morphological data sets. In: Mindell D, ed. *Avian molecular evolution and systematics*. San Diego: Academic Press, 173–211.

**Lewis PO. 2001.** A likelihood approach to estimating phylogeny from discrete morphological character data. *Systematic Biology* **50:** 913–925.

**Livezey BC, Zusi RL. 2007.** Higher-order phylogeny of modern birds (Theropoda, Aves: Neornithes) based on comparative anatomy. II. Analysis and discussion. *Zoological Journal of the Linnean Society* **149:** 1–95.

**Maddison WP, Maddison DR. 2018.** *Mesquite: a modular system for evolutionary analysis, Version 3.61*. Available at: http://www.mesquiteproject.org

**Mayr G. 2009.** Paleogene fossil birds. Heidelberg: Springer.

**Miranda-Ribeiro A. 1938.** Notas ornithológicas, Tinamidae. *Revista do Museo Paulista* **23:** 667–788.

**Mitchell KJ, Llamas B, Soubrier J, Rawlence NJ, Worthy TH, Wood J, Lee MSY, Cooper A. 2014.** Ancient DNA reveals elephant birds and kiwi are sister taxa and clarifies ratite bird evolution. *Science* **6186:** 898–900.

**Mundy NI, Unitt P, Woodruff D, 1997.** Skin from feet of museum specimens as a non-destructive source of DNA for avian genotyping. *The Auk* **114:** 126–129.

**Nesbitt S, Clarke J. 2016.** The anatomy and taxonomy of the exquisitely preserved Green River Formation (early Eocene) lithornithids (Aves) and the relationships of Lithornithidae. *Bulletin of the American Museum of Natural History* **406:** 1–91.

**Porzecanski AL. 2003.** *Historical biogeography of the South American aridlands: a molecular phylogenetic study of endemic avian taxa*. Unpublished Doctoral Dissertation, Columbia University in the City of New York. Preview available from ProQuest Dissertations Publishing; full text available from the author.

**Primmer CR, Borge T, Lindell J, Sætre GP. 2002.** Single-nucleotide polymorphism characterization in species with limited available sequence information: high nucleotide diversity revealed in the avian genome. *Molecular Ecology* **11:** 603–612.

**Prum RO, Berv JS, Dornburg A, Field DJ, Townsend JP, Lemmon EM, Lemmon AR. 2015.** A comprehensive phylogeny of birds (Aves) using targeted next-generation DNA sequencing. *Nature* **526:** 569–573.

**Rambaut A. 2014**. *FigTree*. Available at: http://tree.bio.ed.ac.uk/software/figtree/

**Rambaut A**, **Drummond AJ. 2003.** *Tracer: MCMC trace analysis package*. Available at: http://tree.bio.ed.ac.uk/software/tracer/

**Reddy S, Kimball RT, Pandey A, Hosner PA, Braun MJ, Hackett SJ, Han KL, Harshman J, Huddleston CJ, Kingston S, Marks BD, Miglia KJ, Moore WS, Sheldon FH, Witt CC, Yuri T, Braun EL. 2017.** Why do phylogenomic data sets yield conflicting trees? Data type influences the avian tree of life more than taxon sampling. *Systematic Biology* **66:** 857–879.

**Ronquist F**, **Huelsenbeck JP. 2003.** MrBayes 3: Bayesian phylogenetic inference under mixed models. *Bioinformatics* **19:** 1572–1574.

**Sackton TB**, **Grayson P**, **Cloutier A**, **Hu Z**, **Liu JS**, **Wheeler NE**, **Gardner PP**, **Clarke JA**, **Baker AJ**, **Clamp M**, **Edwards SV. 2019.** Convergent regulatory evolution and loss of flight in paleognathous birds. *Science* **364:** 74–78.

**Sick H. 1984.** *Ornitologıa brasileira, Vol. 1*. Brasilia: Editora Universidade de Brasilia.

**Smith JV**, **Braun EL**, **Kimball RT. 2013.** Ratite non-monophyly: independent evidence from 40 novel loci. *Systematic Biology* **62:** 35–49.

**Stamatakis A. 2014.** RAxML version 8: a tool for phylogenetic analysis and post-analysis of large phylogenies. *Bioinformatics* **30:** 1312–1313.

**Urantówka AD**, **Kroczak A**, **Mackiewicz P. 2020.** New view on the organization and evolution of Palaeognathae mitogenomes poses the question on the ancestral gene rearrangement in Aves. *BMC Genomics* **21:** 874.

**Vizcaıno SF**, **Kay RF**, **Bargo MS. 2012.** A review of the paleoenviroment and paleoecology of the Miocene Santa Cruz Formation. In: Vizcaıno SF, Kay RF, Bargo MS, eds. *Early Miocene paleobiology in Patagonia*. New York: Cambridge University Press, 331–336.

**Woodburne MO**, **Goin FJ**, **Bond M**, **Carlini AA**, **Gelfo JN**, **Lopez GM**, **Iglesias A**, **Zimicz AN. 2014.** Paleogene land mammal faunas of South America; a response to global climate changes and indigeneous floral diversity. *Journal of Mammal Evolution* **21:** 1–73.

**Worthy TH**, **Scofield RP. 2012.** Twenty-first century advances in knowledge of the biology of moa (Aves: Dinornithiformes): a new morphological analysis and moa diagnoses revised. *New Zealand Journal of Zoology* **39:** 87–153.

**Worthy TH, Hand SJ, Archer M. 2014.** Phylogenetic relationships of the Australian Oligo–Miocene ratite *Emuarius gidju* Casuariidae. *Integrative Zoology* **9:** 148–166.

**Yonezawa T**, **Segawa T**, **Mori H**, **Campos PF**, **Hongoh Y**, **Endo H**, **Akiyoshi A**, **Khono N**, **Nishida S**, **Wu J**, **Jin H**, **Adachi J**, **Kishino H**, **Kurokawa K**, **Nogi Y**, **Tanabe H**, **Mukoyama H**, **Yoshida K**, **Rasoamiaramanana A**, **Yamagishi S**, **Hayashi Y**, **Yoshida A**, **Koike H**, **Akishimomiya F**, **Willerslev E**, **Hasegawa M. 2017.** Phylogenomics and morphology of extinct paleognaths reveal the origin and evolution of the Ratites. *Current Biology* **27:** 68–77.

**Zink RM**, **Pavlova A**, **Rohwer S**, **Drovetski SV. 2006.** Barn swallows before barns: population histories and intercontinental colonization. *Proceedings of the Royal Society B: Biological Sciences* **273:** 1245–1251.

## SUPPORTING INFORMATION

Additional Supporting Information may be found in the online version of this article at the publisher's web-site:

**Appendix S1.** List of phenotypic characters used in the combined analysis.
**Appendix S2.** Phenotypic dataset used in the present analysis.
**Table S1.** List of species used in the molecular analysis and the GenBank accession numbers of the sequences.
**Table S2.** Partition scheme and evolutionary models that best fit the molecular data for the Bayesian inference, as obtained with the PARTITIONFINDER program.
**Figure S1.** Molecular (mitochondrial + nuclear) maximum parsimony tree (outgroup relationships unconstrained). Numbers on branches represent bootstrap values.
**Figure S2.** Molecular (mitochondrial + nuclear) Bayesian inference tree (outgroup relationships unconstrained). Numbers on branches represent clade posterior probabilities.
**Figure S3.** Molecular (mitochondrial + nuclear) maximum likelihood tree (outgroup relationships unconstrained). Numbers on branches represent bootstrap values.
**Figure S4.** Maximum parsimony phylogenetic tree obtained in a combined analysis of molecular and morphological data. Numbers on branches represent bootstrap values.
**Figure S5.** Bayesian inference phylogenetic tree obtained in a combined analysis of molecular and morphological data. Numbers on branches represent clade posterior probabilities.
**Figure S6.** Maximum likelihood phylogenetic tree obtained in a combined analysis of molecular and morphological data. Numbers on branches represent bootstrap values.
**Figure S7.** Relationships obtained using the evolutionary placement algorithm (EPA) approach implemented in the program RAXML for the placement of taxa represented by only morphological data in a phylogenetic backbone obtained based on molecular data alone.

**Figure S8.** Maximum parsimony combined matrix tree including fossil taxa. Numbers on branches represent bootstrap values.
**Figure S9.** Bayesian inference combined matrix tree including fossil taxa. Numbers on branches represent clade posterior probabilities.
**Figure S10.** Maximum likelihood combined matrix tree including fossil taxa. Numbers on branches represent bootstrap values.
**Figure S11.** Dated phylogeny using *Lithornis* calibration, assuming this taxon as sister to Tinamidae and a constraint on outgroup relationships. Numbers on nodes represent median estimated ages (in millions of years), and bars represent their 95% height intervals.
**Figure S12.** Dated phylogeny using *Diogenornis* calibration and a constraint on outgroup relationships. Numbers on nodes represent median estimated ages (in millions of years), and bars represent their 95% height intervals.
**Figure S13.** Distribution of unambiguous synapomorphies recovered in the present analyses. Numbers on branches indicate characters listed in the Supporting Information (Appendix S1).
**Figure S14.** Dated phylogeny using *Lithornis* calibration, assuming this taxon as sister to Tinamidae and a constraint on outgroup relationships. Numbers on nodes represent median estimated ages (in millions of years), and bars represent their 95% height intervals.
**Figure S15.** Dated phylogeny using *Diogenornis* calibration and a constraint on outgroup relationships. Numbers on nodes represent median estimated ages (in millions of years), and bars represent their 95% height intervals.
**Figure S16.** Dated phylogeny using the *RAG2*-only matrix and the *Lithornis* calibration, assuming this taxon is sister to Tinamidae. Outgroup relationships were constrained (see main text). Numbers on nodes represent median estimated ages (in millions of years), and bars represent their 95% height intervals.
**Figure S17.** Dated phylogeny using the *RAG2*-only matrix and the *Diogenornis* calibration. Outgroup relationships were constrained (see main text). Numbers on nodes represent median estimated ages (in millions of years), and bars represent their 95% height intervals.